Construction and Building Materials 261 (2020) 119999

Contents lists available at ScienceDirect

Construction and Building Materials

journal homepage: www.elsevier.com/locate/conbuildmat

On strength and stiffness of screwed-in threaded rods embedded in softwood

Haris Stamatopoulos *, Kjell Arne Malo

Department of Structural Engineering, Norwegian University of Science and Technology (NTNU), Rich. Birkelandsvei 1A, 7491 Trondheim, Norway

HIGHLIGHTS

- Existing literature and design guidelines for threaded rods were reviewed.
- Test results were used to derive expressions for the axial capacity and stiffness.
- Theoretical expressions for the lateral capacity and stiffness were provided.
- Areas where further research is needed were highlighted.

ARTICLE INFO

Article history:
Received 5 January 2020
Received in revised form 18 May 2020
Accepted 17 June 2020

Keywords:
Threaded rod
Diameter
Penetration length
Angle to grain
Density
Withdrawal
EN1995-1-1
European Technical Approval/Assessment (ETA)

ABSTRACT

Screwed-in threaded rods with wood screw threads feature high axial capacity and stiffness and can be used as fasteners in highly resistant and stiff timber connections. The purpose of the present paper is to review the existing literature and design rules in the present version of Eurocode 5 (EN 1995-1-1) and European Technical Assessments, to identify gaps of knowledge and to provide some proposals for the strength and stiffness of threaded rods. A collection of experimental results is used to derive simple expressions for the withdrawal capacity and stiffness. Finally, theoretical expressions for the stiffness and the capacity of laterally-loaded threaded rods are provided.

1. Introduction

Screwed-in threaded rods (i.e. rods with wood screw threads and greater diameters than self-tapping screws) feature high axial capacity and stiffness and they may be a promising alternative to dowel-type fasteners or axially-loaded glued-in rods for highly resistant and stiff connections in timber structures. Experimental tests of connections with threaded rods have shown their potential, see e.g. [1–5]. For self-tapping screws with outer-thread diameters up to 12–14 mm, plenty of research results are available with respect to their capacity [6–13], the spacing [14,15] and failure modes of groups of screws [16–18], to name just a few. Design rules for self-tapping screws can be found in many European Technical Approvals/Assessments (abr. ETAs), see for example [19–22]. However, the available design rules and research results for threaded rods are relatively sparse [23–30].

The present version of Eurocode 5 (EN1995-1-1 [31]) provides design rules for screws in Section 8.7. These rules cover the withdrawal capacity, the pull-through capacity (for screws featuring a head) and the minimum requirements for spacings and end/edge distances. On the contrary, design rules are not provided for buckling and block shear despite the fact that these failure modes are mentioned by EN1995-1-1 [31]. A method for the determination of the buckling resistance can be found in ETAs, e.g. [19–21], however it is only verified for self-tapping screws and not for threaded rods. To the knowledge of the authors, no ETA provides rules for the block shear capacity of threaded rods.

In EN1995-1-1 [31], the withdrawal capacity is determined as function of the diameter, the penetration length, the angle to grain and the withdrawal strength parameter perpendicular to grain, which is only provided for screws with diameter up to 12 mm.

* Corresponding author.
E-mail address: haris.stamatopoulos@ntnu.no (H. Stamatopoulos).

https://doi.org/10.1016/j.conbuildmat.2020.119999
0950-0618/

For threaded fasteners with greater diameters, the withdrawal strength parameter is not provided and a value obtained by testing according to EN14592 [32] shall be used. EN 1995-1-1 [31] does not provide rules for the withdrawal stiffness of screws and threaded rods. The withdrawal stiffness is an important parameter, since screws and threaded rods can be used as fasteners in connections and the stiffness of connections influences the overall stiffness of timber structures. Some expressions which provide the withdrawal stiffness of self-tapping screws can be found in their ETAs, but they cannot be extrapolated for threaded rods [33]. Threaded rods are optimized for axial loading, but they may also be subjected to combined axial and lateral loading. Laterally-loaded threaded fasteners are treated as bolts by EN 1995-1-1 [31]. However, this assumption has not been verified for threaded rods. In conclusion, there is a lack of design rules for threaded rods in timber structures and this is a barrier to their use.

In the present paper, the existing literature and the design rules given by EN 1995-1-1 [31] and some ETAs for screws and threaded rods are reviewed. Areas where further research is needed are identified. A collection of experimental results for threaded rods is used to derive simplified expressions for the withdrawal capacity and stiffness. Moreover, the stiffness and capacity of laterally loaded threaded rods are studied by use of analytical models. The scope of this paper is limited to threaded rods embedded in softwood unidirectional timber elements (e.g. solid timber or glued-laminated timber) and only short-term loading is considered. Therefore, issues such as duration of load or fatigue performance are not addressed here. Glued-in rods are also outside the scope of this paper and the reader is referred to relevant publications, e.g. [34,35].

2. Geometric features of threaded rods

A threaded rod embedded in wood is shown in Fig. 1. Due to the interlocking between the thread and the surrounding wood, threaded rods are optimized to be axially-loaded, i.e. to carry forces parallel to their axis (F_{ax}). However, they may also carry lateral forces (F_v). In contrast to screws, most threaded rods have continuous threads and they do not feature a head or a sharp tip.

The following quantities are of interest:

- The outer-thread diameter d (or diameter for short) and the core diameter d_1. Most threaded rods feature diameters d =16–20 mm, but greater diameters are also possible [27–29]. According to EN14592 [32], the core diameter should not be less than 60% and not more than 90% of the outer-thread diameter, i.e. $0.6 \leq d_1/d \leq 0.9$. For most commercially available threaded rods, the core diameter is 75% of the outer-thread diameter, i.e. $d_1/d = 0.75$. A pre-drilled hole is required to insert a threaded rod in a timber element. The pre-drilling diameter is typically equal to the core diameter.
- The penetration length l, i.e. the threaded length of the rod which is embedded in the wood (denoted l_{ef} in EN 1995-1-1 [31]) The minimum penetration length is $6 \cdot d$ [31].
- The non-embedded length l_0.
- The rod-to-grain angle α, which also the angle between the axial force (F_{ax}) and the grain direction. The angle between the lateral force (F_v) and the grain direction is $\beta = 90^\circ - a$.

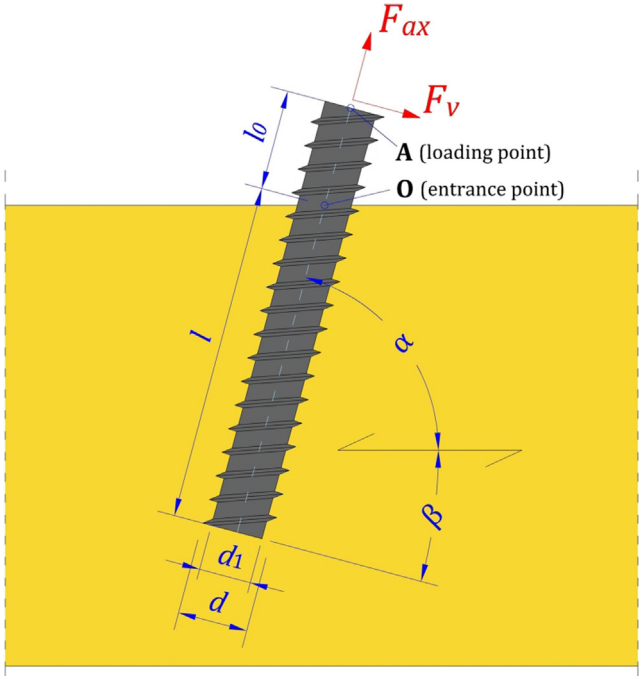

Fig. 1. Geometric features of threaded rods.

3. Axially-loaded threaded rods

3.1. Failure modes

The following failure modes may occur in configurations with axially-loaded threaded fasteners [31]:

- withdrawal failure;
- steel failure, including tear-off failure of the head;
- buckling failure (for fasteners subjected to compression);
- pull-through failure of the head (for fasteners subjected to compression);
- plug shear or block shear in configurations with multiple fasteners;
- splitting failures;

Threaded rods typically feature no head and therefore pull-through and head tear-off failure modes are not relevant and will not be assessed in the present paper. At present, EN 1995-1-1 [31] states that plug shear or block shear shall be taken into account, but no calculation models are provided. Block shear capacity depends on the spacings and therefore capacity predictions should be provided separately for the given configuration with multiple rods. Splitting failures are implicitly addressed by EN 1995-1-1 [31], by use of minimum end/edge distances and spacings and minimum angle to grain, $\alpha \geq 30°$. Considering the failure modes of headless rods not dependent on configuration, the design check for axially-loaded threaded rods is given by Eqs. (1) and (2).

$$\frac{F_{ax,Ed}}{F_{ax,Rd}} \leq 1.0 \tag{1}$$

$F_{ax,Ed}$ is the acting design axial force and $F_{ax,Rd}$ is the design axial resistance, given by:

$$F_{ax,Rd} = \min\left(F_{ax,\alpha,Rd}, F_{t,Rd}\right) \tag{2}$$

This format is similar to the proposal for the design of screws and threaded rods as reinforcements [36]. $F_{ax,\alpha,Rd}$ is the design withdrawal capacity and $F_{t,Rd}$is the design tensile capacity. In addition, for threaded rods subjected to compression, the buckling resistance should also be verified.

Following the EN 1995-1-1 [31] format, the design value for the withdrawal capacity can be written as function of the characteristic value as:

$$F_{ax,\alpha,Rd} = \frac{k_{mod}}{\gamma_M} \cdot F_{ax,\alpha,Rk} \quad (3)$$

where k_{mod} is the modification factor and γ_M is the partial safety factor for connections. The partial safety factor γ_M is a nationally determined parameter; the recommended value is $\gamma_M = 1.3$ [31].

The design tensile capacity $F_{t,Rd}$is given by:

$$F_{t,Rd} = n_{ef} \cdot F_{tens,Rd} \quad (4)$$

The term n_{ef} is the effective number of rods acting together in a connection, further discussed in Section 3.5. $F_{tens,Rd}$ is the design tensile capacity of each rod and according to ETAs (e.g. [20,22]) is obtained by dividing the characteristic tensile capacity $F_{tens,Rk}$with the partial safety factor γ_{M2}:

$$F_{tens,Rd} = \frac{F_{tens,Rk}}{\gamma_{M2}} \quad (5)$$

The partial safety factor γ_{M2} is a nationally determined parameter and the recommended value according to EN 1993-1-1 [37] is $\gamma_{M2} = 1.25$. The design buckling resistance (per rod) $F_{ki,Rd}$is given by Eq. (6) [38] (also given in some ETAs, e.g. [20]):

$$F_{ki,Rd} = \frac{F_{ki,Rk}}{\gamma_{M1}} \quad (6)$$

$F_{ki,Rk}$ is the characteristic buckling resistance, further discussed in Section 3.4. The safety factor γ_{M1} is a nationally determined parameter (the recommended value by EN 1993-1-1 [37] is $\gamma_{M1} = 1.0$).

3.2. Withdrawal properties

Table 1 presents a collection of experimental results which is used to evaluate the withdrawal properties of single threaded rods. It consists of results by Blaß and Krüger [23] (for rods with thread as specified by DIN7998 [39]) and Stamatopoulos and Malo [24–26] (for rods according to [40] with thread also as specified by DIN7998 [39]).

The results cover both the withdrawal capacity and the withdrawal stiffness at reference climatic conditions ($MC \approx 12\%$). The collection consists of 221 test results in total, arranged in 31 sets according to the varied parameters: the diameter, the angle to grain and the penetration length. Based on these parameters, each set is denoted as $S_{d-\alpha-l}$. The number of test results per set (n_{tests}) is at least five. The mean withdrawal capacity and stiffness, the corresponding coefficients of variation (abbr. *CoV*) and the characteristic 5%-fractile withdrawal capacity according to EN14358 [42] are also provided in Table 1 for each set. The fitting of equation predictions (f) to the experimental results (y,with a mean value $\bar{y}$) was evaluated by the Pearson correlation coefficient (abbr. *PCC*) and the coefficient of determination defined as $R^2 = 1 - \sum (y_i - f_i)^2 / \sum (y_i - \bar{y})^2$.

3.2.1. Withdrawal capacity

3.2.1.1. Current European regulations and comparison to experimental results. According to the present version of EN 1995-1-1 [31], the characteristic withdrawal capacity for threaded fasteners embedded in softwood with $d > 12$ mm is given by:

$$F_{ax,\alpha,Rk} = \frac{n_{ef} \cdot f_{ax,k} \cdot d \cdot l}{1.2 \cdot \cos^2\alpha + \sin^2\alpha} \cdot \left(\frac{\rho_k}{\rho_a}\right)^{0.8} \quad (7)$$

Table 1
Collection of experimental results from withdrawal tests of single threaded rods.

Set name	Ref.	n_{tests}	d (mm)	a (deg)	l (mm)	ρ_m (kg/m^3)	ρ_k[a] (kg/m^3)	$F_{ax,\alpha,Rm}$(kN)	CoV_F (%)	$F_{ax,\alpha,Rk}$[b](kN)	$K_{ser,ax}$ (kN/mm)	CoV_K (%)
S16-45-200	[23]	10	16	45	200	430	359	45.6	10.9	36.3	32.4	21.5
S16-45-400		10	16	45	400	433	361	92.4	6.5	80.8	44.3	8.5
S20-45-200		10	20	45	200	431	359	56.6	10.9	44.9	37.7	16.3
S20-45-400		10	20	45	400	433	361	117.3	7.1	101.0	57.7	11.7
S16-90-200		10	16	90	200	422	352	37.4	8.5	31.1	18.2	11.6
S16-90-400		10	16	90	400	441	368	94.1	6.1	83.0	29.7	11.7
S20-90-200		10	20	90	200	425	354	47.9	7.5	40.9	22.6	11.6
S20-90-400		10	20	90	400	441	368	115.1	3.9	103.6	37.8	5.6
S20-90-100	[24–26]	10	20	90	100	472	394	28.0	11.7	21.7	29.0[c]	31.1
S20-90-250		5	20	90	250	472	394	73.2	2.8	64.7	-	-
S20-90-300		5	20	90	300	487	406	96.5	7.2	80.8	61.4	11.2
S20-90-450		5	20	90	450	486	405	139.2	5.3	121.9	66.6	16.4
S20-60-100		6	20	60	100	476	396	28.7	17.3	18.3	36.6[c]	33.2
S20-60-300		5	20	60	300	488	407	93.6	12.3	66.9	73.5	17.3
S20-60-450		5	20	60	450	476	397	141.7	3.1	125.3	90.1	9.4
S20-30-100		10	20	30	100	478	399	27.9	13.0	20.9	42.6[c]	27.5
S20-30-300		5	20	30	300	477	397	99.9	10.7	77.4	111.2	11.2
S20-30-450		5	20	30	450	475	396	144.6	9.2	115.5	100.3	10.5
S20-20-100		10	20	20	100	477	398	30.2	18.9	19.5	53.8[c]	23.1
S20-20-300		5	20	20	300	478	398	98.7	10.8	74.3	116.1	11.4
S20-20-450		5	20	20	450	473	394	145.8	6.3	124.7	121.7	16.0
S20-10-100		10	20	10	100	468	390	25.8	17.7	17.9	56.0[c]	27.4
S20-10-300		5	20	10	300	479	399	99.8	9.8	76.9	126.9	9.8
S20-10-450		5	20	10	450	446	372	127.5	13.8	88.7	132.8	21.9
S20-0-100		10	20	0	100	456	380	26.2	13.9	19.6	54.6[c]	15.9
S20-0-300		5	20	0	300	474	395	89.7	11.7	66.8	121.0	30.1
S20-0-450		5	20	0	450	458	382	130.2	23.9	66.7	121.8	13.0
S20-0-600		5	20	0	600	443	369	161.6	5.2	141.8	128.6	17.4
S20-10-600[d]		5	20	10	600	462	385	–	–	–	131.1	5.3
S20-20-600[d]		5	20	20	600	481	401	–	–	–	128.0	14.3
S20-30-600[d]		5	20	30	600	486	405	–	–	–	114.8	11.2

[a] the characteristic density was determined by $\rho_k = \rho_m/1.2$ [41].
[b] the characteristic withdrawal capacity was determined according to EN14358 [42].
[c] in these sets, mean stiffness values were calculated based on five tests (no stiffness data for the rest of the tests in the set).
[d] in these sets, steel failure was observed so withdrawal capacity was undetermined.

As suggested by Eq. (7), the term $f_{ax,k}$ is the characteristic withdrawal strength parameter for fasteners inserted perpendicular to grain. In contrast to screws with $d \leq 12$ mm, EN 1995-1-1 [31] does not provide a generic expression for the withdrawal strength parameter, which should instead be determined by testing for an associated characteristic density ρ_a. The term $(\rho_k/\rho_a)^{0.8}$ is used to adjust the withdrawal strength to the characteristic density ρ_k. According to ETA-12/0114 [19], Eq. (7) applies for threaded rods with d =16 mm by use of $f_{ax,k}$ = 10.0 N/mm^2 for ρ_a = 350 kg/m^3. For these values of and for a single fastener ($n_{ef} = 1.0$), Eq. (7) reduces to:

$$F_{ax,\alpha,Rk} = \frac{10 \cdot d \cdot l}{1.2 \cdot \cos^2\alpha + \sin^2\alpha} \cdot \left(\frac{\rho_k}{350}\right)^{0.8} \tag{8}$$

According to some ETAs, e.g. [20,21] the characteristic withdrawal capacity of a single threaded rod embedded in solid timber and laminated timber products is given by:

$$F_{ax,\alpha,Rk} = n_{ef} \cdot k_{ax} \cdot f_{ax,k} \cdot d \cdot l \cdot \left(\frac{\rho_k}{\rho_a}\right)^{0.8} \tag{9}$$

$$k_{ax} = \begin{cases} 1.0, 45^\circ \leq \alpha \leq 90^\circ \\ 0.30 + 0.70 \cdot a/45^\circ, 0^\circ \leq \alpha < 45^\circ \end{cases} \tag{10}$$

Here, the effect of the angle to grain on the withdrawal capacity is taken into account by use of a bi-linear expression (Eq.(10)), similarly to proposals found in the literature [8,10,13]. According to experimental results for threaded rods [26] also used in this study, the ratio between the characteristic withdrawal strength perpendicular to grain and parallel to grain (i.e. $f_{ax,k,\alpha=90^\circ}/f_{ax,k,\alpha=0^\circ}$) was 1.17 which is in very good agreement with Eq. (8). Eq. (10) overestimates severely this value. Therefore, only Eq. (8) was chosen for comparison to experimental results.

Fig. 2 shows the correlation between the prediction by Eq. (8) and the experimental characteristic capacities in Table 1. Individual test results have also been added to this plot; the predictions for individual tests have been calculated by use of Eq. (8) and the characteristic density of the set they belong to. Eq. (8) generally provides safe-side predictions, however it overestimates the characteristic capacity for some sets with small penetration length and for the set S20-0-450 which has a low characteristic capacity.

It is evident that Eq. (8) becomes quite conservative for increasing values of the characteristic withdrawal capacity. This trend in

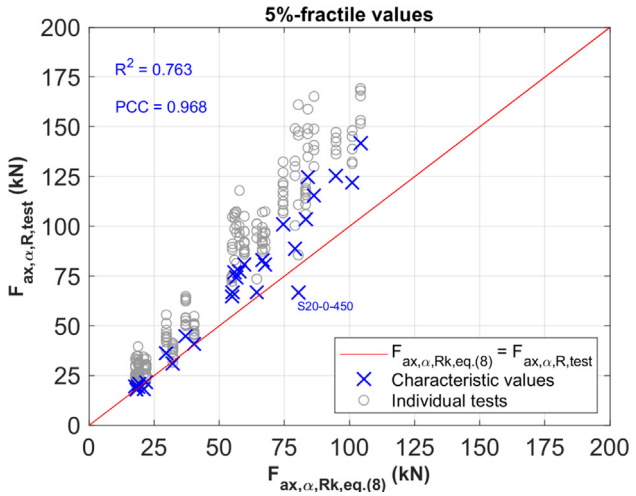

Fig. 2. Correlation between experimental characteristic withdrawal capacity and Eq. (8).

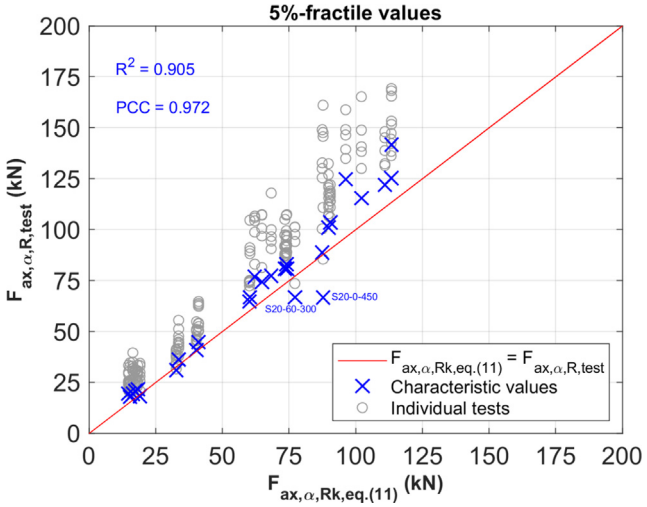

Fig. 3. Correlation between experimental characteristic withdrawal capacity and Eq. (11).

Fig. 2 is observed because the withdrawal strength parameter (i.e. $f_{ax,\alpha} = F_{ax,\alpha,R}/d \cdot l$) increases for increasing penetration length. This observation is, at first, non-intuitive. One would expect that $f_{ax,\alpha}$ should decrease for increasing length because of non-uniform withdrawal stress distribution. At best, $f_{ax,\alpha}$ could be constant for uniform withdrawal stress distribution. Analytical models based on Volkersen theory [43] suggest that the withdrawal stress distribution in screwed-in threaded rods is highly non-uniform for small loads [24], but nearly uniform at failure [25]. But why is $f_{ax,\alpha}$ not constant, but increasing for increasing length? This observation may be explained by the fact that the withdrawal stress is zero at the entrance point and therefore some length is required to build-up. This assumption is further supported by experimental results on partially threaded self-tapping screws [6,8] where a higher capacity was obtained if the thread was embedded by up to $2 \cdot d$, compared to the capacity of screws with non-embedded thread.

3.2.1.2. Regression analysis of the experimental results. The collection of experimental results was used to derive an expression for the characteristic withdrawal capacity by use of non-linear regression analysis. Therefore, the derived expression applies within the range of parameters given in Table 1. The basic format of Eq. (8) was maintained and an attempt was made to fit well the experimental capacities, but also to keep the prediction on the safe side as much as possible. The aforementioned effect of the penetration length on the withdrawal strength was taken into account by use of a length-reduction factor $k_{length,F}$. The analysis resulted in Eqs. (11)–(13) (units: $F_{ax,\alpha,Rk}$ in N, d and l in mm, $f_{ax,k}$ in N/mm^2, ρ_k in kg/m^3). The correlation between the prediction by Eq. (11) and the experimental results is shown in Fig. 3.

$$F_{ax,\alpha,Rk} = \frac{f_{ax,k} \cdot d \cdot l}{1.2 \cdot \cos^{2.3}\alpha + \sin^{2.3}\alpha} \tag{11}$$

$$f_{ax,k} = 12.2 \cdot \left(\frac{d}{20}\right)^{-0.1} \cdot \left(\frac{\rho_k}{400}\right)^{0.9} \cdot k_{length,F} \tag{12}$$

$$k_{length,F} = \min\left[0.6 + 0.4 \cdot \frac{l}{250}, 1.0\right] \tag{13}$$

Compared to Eq. (8), Eq. (11) provides a better fit to the experimental results and a safe-side prediction for small penetration lengths, but it overestimates the characteristic capacity for sets

S20-60-300 and S20-0-450. Eq. (14) is a very conservative expression obtained by multiplying Eq. (8) with the length-reduction factor by Eq. (13). Fig. 4 shows the correlation between the predictions by Eq. (14) and the experimental results. The only overestimated value in Fig. 4 belongs to set S20-0-450, i.e. for a set with $\alpha = 0^{\circ}$ which is not allowed by EN 1995-1-1 [31].

$$F_{ax,\alpha,Rk} = \frac{10 \cdot d \cdot l}{1.2 \cdot \cos^2\alpha + \sin^2\alpha} \cdot k_{length,F} \cdot \left(\frac{\rho_k}{350}\right)^{0.8} \quad (14)$$

Regression analysis was also used to derive a simplified expression for the mean withdrawal capacity $F_{ax,\alpha,Rm}$ (units: $F_{ax,\alpha,Rm}$ in N, d and l in mm, ρ in kg/m^3):

$$F_{ax,\alpha,Rm} = 15.0 \cdot d \cdot l \cdot \left(\frac{\rho_m}{470}\right) \quad (15)$$

The experimental results did not show a very clear effect of the angle α on the mean values of the withdrawal capacity; hence angle was excluded as a parameter in Eq. (15). The angle to grain has mostly an effect on the variability of the withdrawal capacity and therefore it appears as a parameter in the determination of characteristic values. The correlation between the predictions by Eq. (15) and test results is shown in Fig. 5. Values for individual experimental results, calculated by use of the individual density instead of ρ_m in Eq. (15), have also been added in Fig. 5.

3.2.1.3. Considerations about the angle to grain direction. EN 1995-1-1 [31] does not allow axially-loaded screws installed at an angle to grain smaller than 30°, i.e. $\alpha \geq 30^{\circ}$. Axially-loaded fasteners inserted at small angles to grain induce tensile stresses perpendicular to grain in the surrounding timber. Moreover, connections with fasteners oriented parallel to grain might be vulnerable to cracks along the grain, since a single crack along the grain might lead to a considerable loss of strength if the crack and the fastener coincide. Such cracks can occur, for instance, due to moisture-induces stresses. Therefore, threaded rods parallel to the grain direction ($\alpha = 0^{\circ}$) should be avoided.

On the contrary, threaded rods installed at an inclination to the grain can bridge cracks along the grain, transfer forces and prevent crack propagation. An example is shown in the moment-resisting connection in Fig. 6 which failed due to shear failure in the column. The threaded rod at the bottom edge of the beam (inserted at an angle of 10°) bridged the crack along the grain, maintaining the structural integrity of the beam. The longer the rods, the smaller

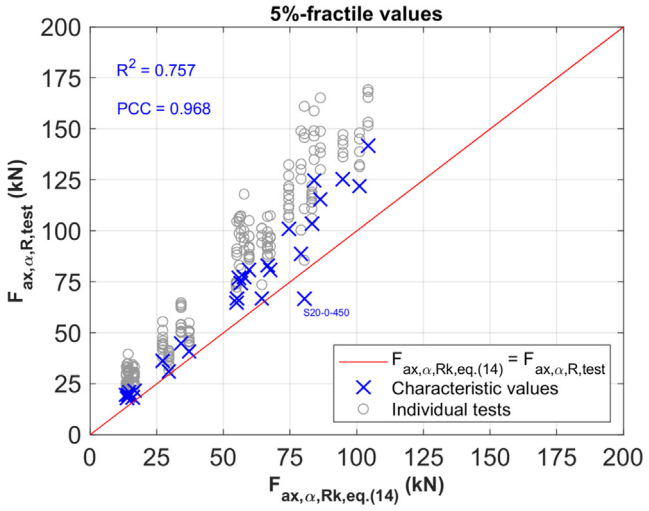

Fig. 4. Correlation between experimental characteristic withdrawal capacity and Eq. (14).

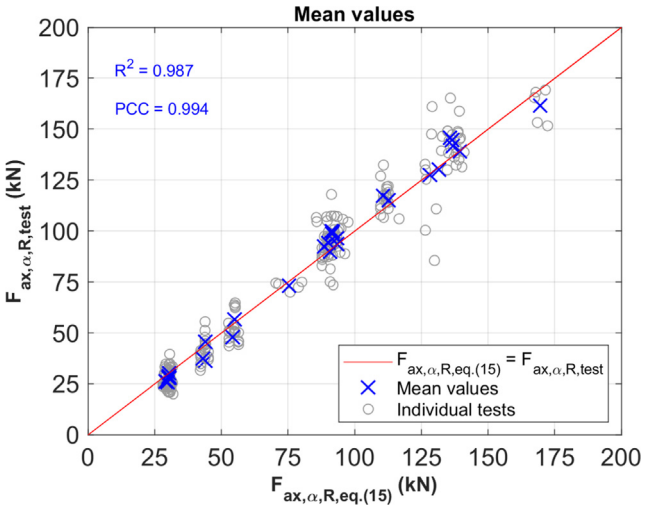

Fig. 5. Correlation between mean experimental withdrawal capacity and prediction by Eq. (15).

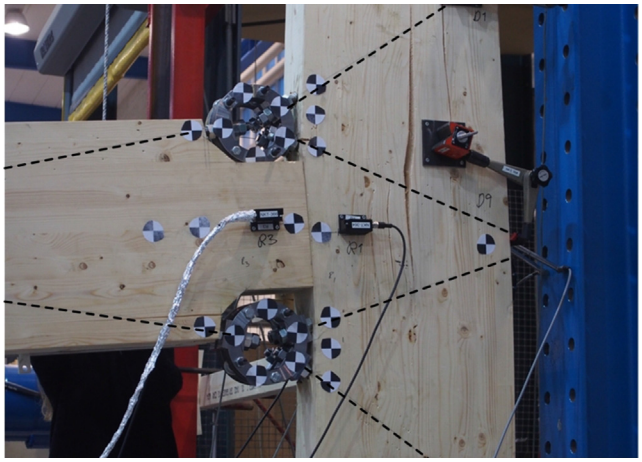

Fig. 6. Moment-resisting connection with threaded rods (dashed-lines) [2].

the inclination might be allowed, since longer rods can bridge more fibers. It is therefore the opinion of the authors that the minimum allowed inclination of axially-loaded threaded rods should be a function of the penetration length and vice-versa. This is reflected in existing recommendations in some ETAs, e.g. [20,21] where the minimum penetration length is given as function of angle α:

$$l \geq \min(4 \cdot d/\sin\alpha, 20 \cdot d) \quad (16)$$

Furthermore, there is experimental indication that threaded rods inserted at small angles to the grain in timber beams subjected to bending (e.g. like the beam in Fig. 6), show lower withdrawal strength compared to the reference pure withdrawal conditions, see [3,44]. To take this into account, a reduced withdrawal strength may be considered for threaded rods with small inclination to grain in elements subjected to bending. Due to lack of more data, a conservative assumption would be to use half of the withdrawal strength, i.e. $f_{ax,k}/2$. Finally, experimental tests have shown that axially-loaded screws inserted parallel to grain have poor long-term properties [45]. However, the validity of this observation needs to be checked for threaded rods and for other (small) angles to the grain.

3.2.1.4. Effect of moisture content. To the knowledge of the authors, there is no systematic study of the effect of varying moisture content ($MC \neq 12\%$) on the withdrawal properties of threaded rods. Based on experiments with self-tapping screws at different moisture contents, Ringhofer et al. [46] provided the following simplified estimation for the effect of moisture content on withdrawal strength (MC in %):

$$k_{MC} = \frac{f_{ax,\alpha,R,MC}}{f_{ax,\alpha,R,12\%}} = \begin{cases} 1.0 & 8\% \le MC \le 12\% \\ 1.0 - 0.034 \cdot (MC - 12) & 12\% < MC \le 20\% \end{cases} \quad (17)$$

The factor 0.034 in Eq. (17) represents the strength reduction for 1% increase of moisture content above 12%. In [46], this factor was 0.036 and 0.031 for screws inserted parallel and perpendicular to grain, respectively. The value 0.034 is a simplification, so that Eq. (17) applies for both angles. Applying Eq. (17) for $MC \approx 20\%$ (i.e. Service Class 3), results in $k_{MC} = 0.73$, i.e. the strength is 73% of the reference strength. In EN 1995-1-1 [31], the strength reduction due to increasing moisture content is included in the modification factor k_{mod}. Assuming short-term loading for glulam and solid timber, we get $k_{mod} = 0.9$for Service Classes 1 and 2 and $k_{mod} = 0.7$ for Service Class 3. Therefore, in Service Class 3, the strength will be $0.7/0.9 = 0.78$ times the strength in Service Classes 1, 2. This ratio varies between 0.78 and 0.83 for the various load-duration classes. Compared to Eq. (17), EN 1995-1-1 [31] is always non-conservative, especially for screws inserted parallel to grain.

3.2.2. Withdrawal stiffness

Axially-loaded threaded rods are stiff fasteners and due to lack of clearance they allow immediate load take-up, i.e. no initial slip occurs for small loads [24]. These properties make them ideal fasteners for stiff connections in timber structures. At present, EN 1995-1-1 [31] provides no rules for the withdrawal stiffness ($K_{ser,ax}$) of screws or threaded rods and this is a limitation for their use as fasteners. Some expressions can be found in ETAs. For example:

- ETA-11/0024 [21] (the first equation is based on [11]) ($K_{ser,ax}$ in N/mm, l and d in mm):

$$K_{ser,ax} = \begin{cases} 780 \cdot l^{0.4} \cdot d^{0.2}, Self - tapping\ \ screws, d \le 12\ \ mm \\ 250 \cdot l, Threaded\ \ Rods \end{cases} \quad (18)$$

- ETA-11/0030 [20] for self-tapping screws or threaded rods ($K_{ser,ax}$ in N/mm, l and d in mm):

$$K_{ser,ax} = 25 \cdot l \cdot d \quad (19)$$

Analytical models, finite element analysis and experimental results [24] have shown that the withdrawal stiffness is a highly non-linear function of the penetration length l; it is approximately linearly dependent on the penetration length for small values of l, whereas for long rods (approx. $l \ge 15 \cdot d$), it converges to an upper limit value [24], i.e. the withdrawal stiffness of a semi-infinite rod. The withdrawal stiffness depends also on the angle to grain and the diameter (as indicated by the stiffness values in Table 1), as well as the material properties of wood. Eqs. (18) and (19) do not take some of these parameters and dependencies into account and their predictions can deviate significantly from the experimental results [33]. The dependence of withdrawal stiffness on material properties may be considered in a simplified way by use of density as parameter. Analytical models and Finite Element analysis [24,47] show that the withdrawal stiffness is also dependent on the loading conditions (e.g. pull-pull, pull-push, pull-shear).

Equation (20) was derived by non-linear regression analysis on the experimental results in Table 1 (units: $K_{ser,ax}$ in N/mm, d and l in mm, ρ_m in kg/m^3). However, the available experimental results in Table 1 come from different test set-ups. In these set-ups, there are differences in the measurement of the relative timber-to-rod deformation and therefore there is no consensus on the experimental determination of the withdrawal stiffness values. Having these uncertainties in mind, Eq. (20) is much more accurate than Eqs. (18) and (19), but it still has an approximate nature and should be used within the range of parameters (e.g. density, diameter) for which it has been derived, see Table 1. The correlation between Eq. (20) and mean and individual experimental results is shown in Fig. 7.

$$K_{ser,ax} \approx \frac{50000 \cdot \left(\frac{d}{20}\right)^2 \cdot \left(\frac{\rho_m}{470}\right)^2 \cdot k_{length,K}}{0.40 \cdot \cos^{2.3}\alpha + \sin^{2.3}\alpha} \quad (20)$$

$$k_{length,K} = \min\left[\left(\frac{l}{300}\right)^{0.75}, 1.0\right] \quad (21)$$

The total axial stiffness at the loading point A (see Fig. 1), considering the free length of the rod is given by Eq. (22), where $K_{ax,l0} = A_s \cdot E_s / l_0$, $A_s \approx \pi \cdot {d_1}^2/4$ and $E_s = 210,000$MPa for steel.

$$K_{ser,ax,tot} = \frac{K_{ser,ax} \cdot K_{ax,l0}}{K_{ser,ax} + K_{ax,l0}} \quad (22)$$

3.3. Tensile capacity

The characteristic tensile capacity $F_{tens,Rk}$ is typically provided by the ETAs. Screws and threaded rods are hardened during rolling of their thread, resulting in higher capacity and lower ductility. In [25,44,48], for a sample of 28 steel failures of threaded rods with $d = 20$ mm from the same manufacturer [40] (different deliveries), the mean tensile capacity of the rods was 173 kN and the coefficient of variation was less than 5.0%. The characteristic tensile capacity according to the manufacturer [40] was 145 kN, i.e. $F_{tens,Rd} = 116.0$ kN for $\gamma_{M2} = 1.25$ by use of Eq. (5). These results suggest that Eq. (5) may be conservative and the use of a smaller safety factor might be considered.

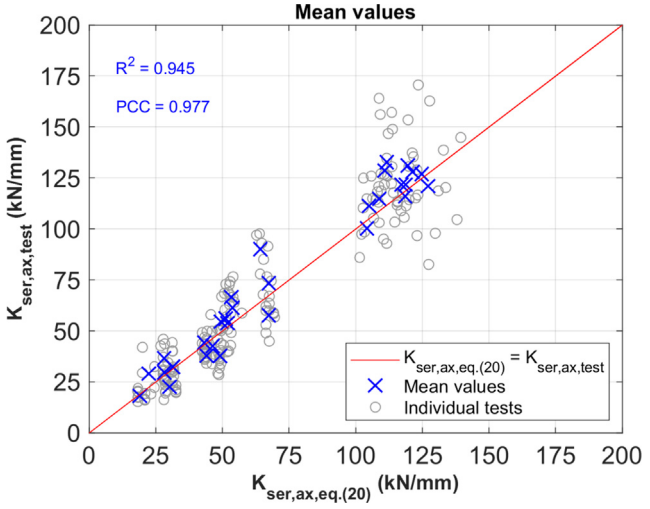

Fig. 7. Correlation between experimental mean withdrawal stiffness and prediction by Eq. (20).

3.4. Buckling resistance

In the present version of EN 1995-1-1 [31], there are no design rules for the buckling resistance of screws and threaded rods. Such rules can be found for self-tapping screws in ETAs, e.g. [19–21], based on the work of Blaß and Bejtka [38]. The buckling resistance of a screw subjected to compression is obtained as a fraction of the axial capacity of the screw:

$$F_{ki,Rk} = \kappa_c \cdot N_{pl,k} \tag{23}$$

The yielding strength of the $f_{y,k}$ is used here to determine the axial capacity:

$$N_{pl,k} = f_{y,k} \cdot \pi \cdot {d_1}^2/4 \tag{24}$$

The factor κ_c is calculated as function of the relative slenderness $\overline{\lambda}_k$ as follows:

$$\kappa_c = \begin{cases} 1 & \overline{\lambda}_k \le 0.2 \\ 1/\left(k + \sqrt{k^2 - {\overline{\lambda}_k}^2}\right) & \overline{\lambda}_k > 0.2 \end{cases} \tag{25}$$

$$k = 0.5 \cdot \left[1 + 0.49 \cdot \left(\overline{\lambda}_k - 0.2\right) + {\overline{\lambda}_k}^2\right] \tag{26}$$

$$\overline{\lambda}_k = \sqrt{N_{pl,k}/N_{ki,k}} \tag{27}$$

The ideal elastic buckling load $N_{ki,k}$ is given as function of the characteristic value of the foundation modulus k_v and the bending stiffness $E_s \cdot I_s$:

$$N_{ki,k} = \sqrt{k_{v,\alpha,k} \cdot E_s \cdot I_s} \tag{28}$$

where $I_s \approx \pi \cdot {d_1}^4/64$ is the second moment of area of the screw and $k_{v,\alpha,k}$is the characteristic value of the foundation modulus as function of the angle α (units: $k_{v,\alpha,k}$ in N/mm^2,d in mm,ρ_k in kg/m^3):

$$k_{v,\alpha,k} = (0.19 + 0.012 \cdot d) \cdot \rho_k \cdot \left(\alpha/180^\circ + 0.50\right) \tag{29}$$

An expression for the foundation modulus of self-tapping screws with $d \le$12 mm can also be found in [49] as function of angle β (units: $k_{v,\beta}$ in N/mm^2,d in mm,ρ in kg/m^3):

$$k_{v,\beta} = \frac{(0.22 + 0.014 \cdot d) \cdot \rho}{1.17 \cdot \sin^2\beta + \cos^2\beta} \tag{30}$$

To the knowledge of the authors, these equations have not been experimentally verified for threaded rods. It is evident that other factors can influence the buckling resistance, e.g. the free length of the rod $l_0$or whether the rotation of the rod is restrained or not at the entrance point. Moreover, the value of the foundation modulus k_v remains unknown for threaded rods and Eqs. (29) and (30) have not been experimentally verified for $d \ge$12 mm.

3.5. Configurations with multiple axially-loaded threaded rods

3.5.1. Effect of end/edge distances and spacings and number of fasteners

The effectiveness of connections with multiple axially-loaded fasteners may be influenced by insufficient edge and end distances or spacings, since failure modes other than withdrawal or steel failure may be triggered and the full axial capacity may not be reached. To take this into account, restrictions apply with respect to minimum edge and end distances and fastener spacings. The minimum edge and end distances and spacings for screws according to EN 1995-1-1 [31] are provided in Table 2 and the associated definitions are specified in Fig. 8. The minimum requirements given by ETAs are typically less strict, see e.g. the values provided by [19,20] in Table 2. As shown in Fig. 8, fasteners may be inserted in rows parallel to the same plane of the grain (e.g. fasteners 1-3-5 and 2-4-6) or in different grain planes (e.g. fasteners 1–2, 3–4 and 5–6).

Table 2
Minimum end/edge distances and spacings for screws or threaded rods.

Spacing/ Distance	EN 1995-1-1 [31]	ETA-12/0114 [19]	ETA-11/0030 [20]
a_1	$7 \cdot d$	$5 \cdot d$	$5 \cdot d$
$a_{1,CG}$	$10 \cdot d$	$5 \cdot d$	$10 \cdot d$
a_2	$5 \cdot d$	$2.5 \cdot d$ if $a_1 \cdot a_2 \ge 25 \cdot d^2$	$5 \cdot d$(or $2.5 \cdot d$ if $a_1 \cdot a_2 \ge 25 \cdot d^2$)
$a_{2,CG}$	$4 \cdot d$	$4 \cdot d$	$4 \cdot d$

According to EN 1995-1-1 [31], the effective number n_{ef} of axially-loaded fasteners acting together in a connection is given as function of the total number of fasteners n, as follows:

$$n_{ef} = n^{0.9} \tag{31}$$

In some ETAs, e.g. [19,20], a modified effective number is used (based on [50]):

$$n_{ef} = \max(n^{0.9}, 0.9 \cdot n) \tag{32}$$

In the case of multiple axially-loaded threaded rods, available experimental results are very sparse. Fig. 9 summarizes the experimentally recorded effectiveness per fastener (i.e. n_{ef}/n) for threaded rods [29,30] and also for self-tapping screws [17,18,50].

Mori et al [29] presented an experimental study of configurations with 1, 2 and 4 threaded rods ($d = 25$ mm, $l = 200$ mm) inserted parallel and perpendicular to the grain with varying spacings in glulam elements made of pine. For rods inserted parallel to grain, the effective number of fasteners n_{ef} (based on mean values) was higher than the predicted by Eqs.(31)-(32), with the exception of specimens with 2 rods at spacing $2d$ (*underlier1* in Fig. 9). Similar tests for screws and glued-in rods inserted parallel to grain in softwood, have shown that a minimum spacing of $5d$ is required to achieve full capacity [14,51]. In tests with rods inserted perpendicular to grain by Mori et al [29], the effective number of rods (n_{ef}) inserted in the same plane of grain was lower than the prediction by Eqs.(31)-(32) for both tested spacings $a_1 = 2d$ and $a_1 = 4d$ (*underliers2* in Fig. 9). On the contrary, specimens with rods inserted in different grain planes showed greater n_{ef} values than the predicted by Eqs.(31)-(32), even for the smallest used spacing, which was $a_2 = 2d$. A similar observation has been made in tests by Stamatopoulos and Malo [30] for threaded rods (d =20 mm, l =450 mm) with spacing $a_2 = 2d$ inserted at an angle of 60° and 90° to the grain direction. However, for smaller angles to grain $(15, 30^\circ)$ and spacing $a_2 = 2d$ the values of n_{ef} were smaller than the prediction by Eqs. (31)–(32) (*underliers3* in Fig. 9). In the same study [30], specimens with small edge distances ($a_{2,CG} = 1.5 \cdot d$) showed similar capacity for rod-to-grain angles 60° and 90° and higher capacity for rod-to-grain angles 15° and 30°, compared to the results for small spacing $a_2 = 2d$. With respect to withdrawal stiffness in [30], all configurations with a pair of rods inserted in different grain planes showed no significant group effect, i.e. the effective number of rods ($n_{ef,ser}$) under service load was found to be approximately equal to the number of rods, i.e. $n_{ef,ser} \approx n \approx 2$.

Fig. 9 also presents the effectiveness per fastener of configurations with multiple self-tapping screws embedded in spruce elements. These results are obtained from tests performed by Krenn and Schickhofer [50] ($d = 8$mm, $\alpha = 30/45^\circ$, $n = 1 - 8$) and Mahlknecht et al [17,18] ($d = 6, 8$mm, $\alpha = 90^\circ$, $n = 1, 4 - 16$). In the former study [50], the distances and spacings complied with the minimum requirements in their ETA and n_{ef}/n was determined

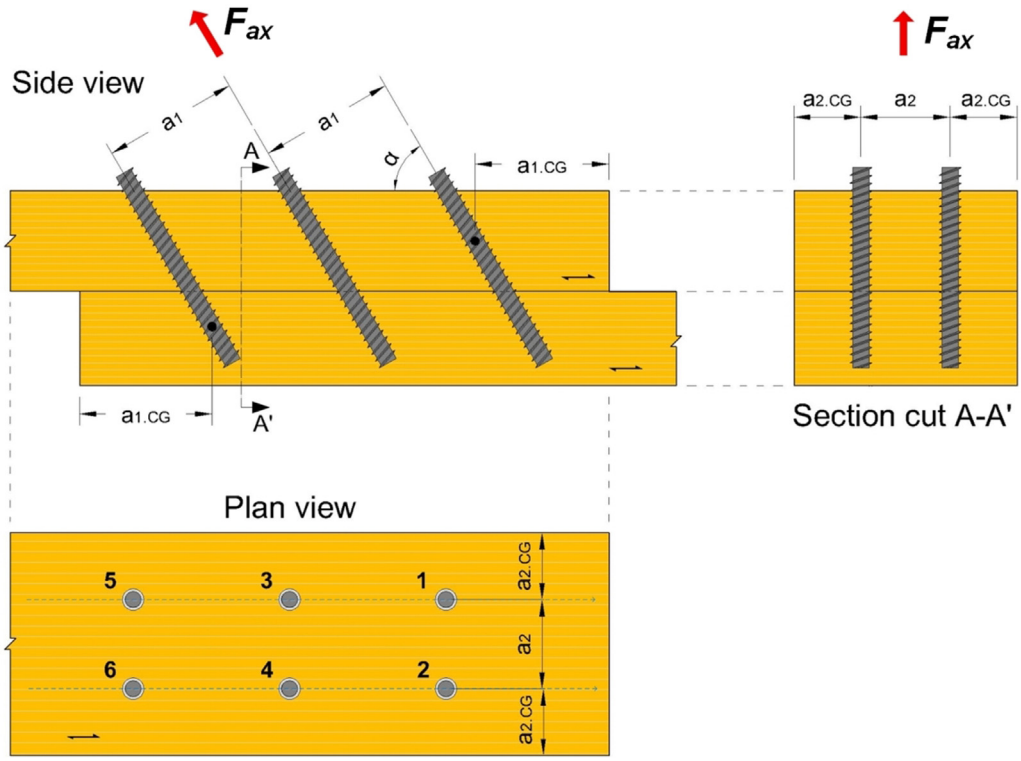

Fig. 8. Definitions of edge and end distances and spacings according to EN 1995-1-1 [31].

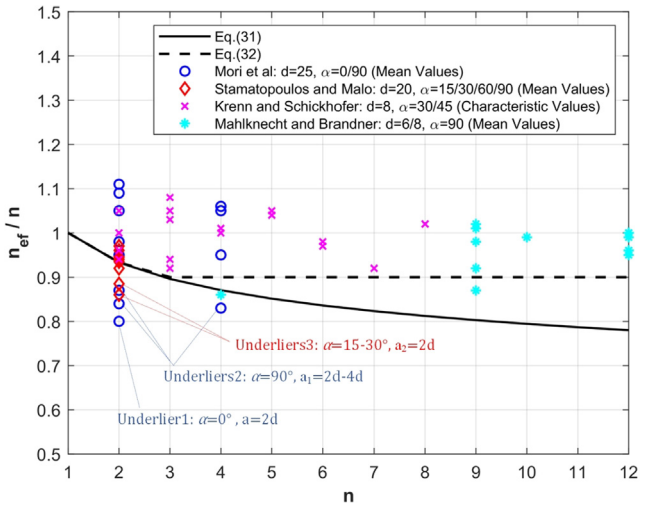

Fig. 9. Effectiveness per fastener in connections with multiple axially-loaded screws or rods.

by use of 5%-fractile values. In the latter study [17,18], the spacings were varied and n_{ef}/n was determined by use of mean values. Both experimental studies concluded that Eqs. (31) and (32) provide a generally safe-side prediction, see also Fig. 9. This observation was made for different failure modes (withdrawal, tensile failure, head tear-off). Tests results show that n_{ef}/n tends to be close to 1.0 as n increases, i.e. a homogenization effect takes place (increasing number of fasteners result in lower variability). With respect to stiffness, a group effect was identified by Krenn and Schickhofer [50] and an effective number of screws under service load $n_{ef,ser} = n^{0.8}$ was found based on their experimental results. Block shear failures were observed in the experiments by Mahlknecht et al [17,18] at spacings allowed by EN 1995-1-1 [31] and ETAs. Since the fulfilment of spacing requirements does not exclude block shear, it should be considered separately as a potential failure mode.

In conclusion, experimental results show that rods inserted in different grain planes are more effective than rods inserted in the same plane of grain. This finding can be explained by greater stress interactions occurring for fasteners that share the same grain plane, which is reflected in the higher requirements for spacing a_1 compared to a_2. Moreover, configurations with small distance a_1 can potentially result in plug-shear failure [16]. On the contrary, the minimum requirements by EN 1995-1-1 [31] for a_2 and $a_{2.CG}$ seem to be conservative. Finally, the available experimental results suggest that Eqs. (31) and (32) would probably provide a safe-side prediction for configurations with axially-loaded threaded rods which comply with the minimum requirements in Table 2.

3.5.2. Block shear

At present, EN 1995-1-1 [31] provides a method for the determination of the block shear capacity in connections with dowel type fasteners in Annex A. On the other hand, no design rules are provided for the block shear of groups of axially-loaded screws or threaded rods despite the fact that it is a failure mode mentioned by EN 1995-1-1[31]. As mentioned in Section 3.5.1, Mahlknecht et al [17,18] showed that configurations with axially loaded self-tapping screws ($d = 6$, 8 mm) inserted perpendicular to grain can fail due to block shear even if the minimum spacing requirements are fulfilled. The observed failure mode was characterized by severe cracking due to rolling shear and tension perpendicular to grain. In the same work, they proposed an analytical model for the block shear capacity based on the stresses-state of the free-body block defined by the perimeter and the penetration length of the fasteners, see in detail [17]. To the knowledge of the authors, there are no existing experimental results for the block shear of configurations with axially-loaded threaded rods.

For a comprehensive overview of block/plug shear models, the reader is kindly referred to [52].

4. Laterally loaded threaded rods

4.1. Lateral load-carrying capacity

A laterally-loaded threaded rod is shown schematically in Fig. 10a. Laterally-loaded screws with an effective diameter $d_{ef} \geq 6$ mm are treated as bolts by the present version of EN 1995-1-1 [31]. For screws not featuring a smooth shank, d_{ef} is taken as 1.1 times the core diameter and it is used for the determination of the embedment strength and yielding moment (but: the outer-thread diameter is used for the determination of minimum spacings, end and edge distances). By use of d_{ef}, the expressions by EN 1995-1-1 [31] for the characteristic embedment strength $f_{h,k}$ and the yielding moment $M_{y,Rk}$ are respectively (ρ_k in kg/m^3, d_{ef} in mm, $f_{h,k}$ and $f_{u,k}$ in N/mm^2 and $M_{y,Rk}$ in N·mm):

$$f_{h,k} = \frac{0.082 \cdot \rho_k \cdot (1 - 0.01 \cdot d_{ef})}{k_{90} \cdot \sin^2\beta + \cos^2\beta} \tag{33}$$

$$M_{y,Rk} = 0.3 \cdot f_{u,k} \cdot {d_{ef}}^{2.6} \tag{34}$$

For softwood, the factor k_{90} is given by:

$$k_{90} = 1.35 + 0.015 \cdot d_{ef} \tag{35}$$

In some ETAs e.g. [20,21], the embedment strength for screws and threaded rods embedded in pre-drilled holes in softwood is given by Eq. (36) as function of the outer-thread diameter:

$$f_{h,k} = \frac{0.082 \cdot \rho_k \cdot (1 - 0.01 \cdot d)}{2.5 \cdot \cos^2\alpha + \sin^2\alpha} \tag{36}$$

To the knowledge of the authors, there are no experimental results available to verify the validity of Eqs. (33)–(36) for threaded rods subjected to pure lateral loading. Therefore, the necessity for experimental testing of laterally-loaded threaded rods is highlighted.

For long threaded rods, the ductile failure shown in Fig. 10b will occur prior to embedment failure. By assuming perfect plastic behaviour (the same principle as in Johansen's equations [53]), the characteristic lateral load-carrying capacity $F_{v,Rk}$ can be expressed as:

$$F_{v,Rk} = \sqrt{2 \cdot f_{h,k} \cdot d_{ef} \cdot M_{y,Rk} \cdot (1 - n_{M0,y})} \left[+F_{ax,Rk}/4\right] \tag{37}$$

The term $F_{ax,Rk}/4$ is the contribution from the rope effect, which cannot be greater than the Johansen's part [31]. The term $n_{M0,y}$ is the moment at the entrance point M_0 normalized by the characteristic yielding moment ($-1 \leq n_{M0,y} < 1$ for perfect plastic behaviour):

$$n_{M0,y} = M_0 / M_{y,Rk} \tag{38}$$

If the load is applied without eccentricity, i.e. for $l_0 = 0$, the lateral load-carrying capacity depends on whether the rotation is restrained or not, at the entrance point O:

- No eccentricity ($l_0 = 0$), free rotation at O ($n_{M0,y} = 0$)

$$F_{v,Rk} = \sqrt{2 \cdot f_{h,k} \cdot d_{ef} \cdot M_{y,Rk}} \left[+F_{ax,Rk}/4\right] \tag{39}$$

- No eccentricity ($l_0 = 0$), fixed rotation at O ($n_{M0,y} = -1$)

$$F_{v,Rk} = 2 \cdot \sqrt{f_{h,k} \cdot d_{ef} \cdot M_{y,Rk}} \left[+F_{ax,Rk}/4\right] \tag{40}$$

Equations (39) and (40) correspond to the equations by EN 1995-1-1 [31] for steel-to-timber connections with thin and thick steel plates respectively without the adjustments for safety factors; i.e. the factor 1.15 is not included in Eq. (39) and the factor 2 is used in Eq. (40) instead of 2.3. Setting $M_0 = F_{v,Rk} \cdot e_0$ and solving Eq. (37) for $F_{v,Rk}$ results in Eq. (41) [54].

$$F_{v,Rk} = f_{h,k} \cdot d_{ef} \cdot \left(\sqrt{\frac{2 \cdot M_{y,Rk}}{f_{h,k} \cdot d_{ef}} + {e_0}^2} - e_0 \right) \left[+F_{ax,Rk}/4\right] \tag{41}$$

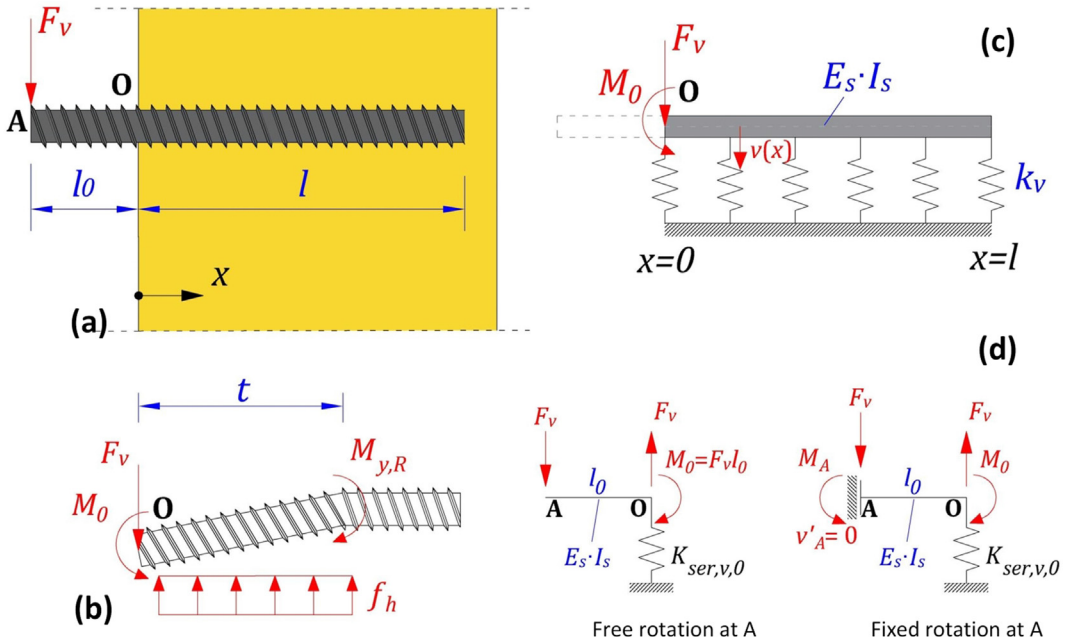

Fig. 10. Laterally-loaded threaded rod (a), ductile failure mechanism (b), modelling of embedded part as a beam on elastic foundation (c), and modelling of the non-embedded part (d).

The value of e_0 depends on whether the rotation at the loading point A is restrained or not:

- Load applied with eccentricity ($l_0 > 0$), free rotation at A ($-1 \leq n_{M0,y} < 1$):

$$e_0 = l_0 \tag{42}$$

- Load applied with eccentricity ($l_0 > 0$), fixed rotation at A ($-1 \leq n_{M0,y} < 1$):

$$e_0 \approx (l_0 - l_c)/2 \tag{43}$$

The term l_c is a characteristic length (see also Appendix A):

$$l_c = \sqrt[4]{4 \cdot E_s \cdot I_s / k_v} \tag{44}$$

The foundation modulus k_v is further discussed in Section 4.2. Eq.(43) is approximate because the moments at points O and A are calculated assuming elastic behaviour, i.e. the softening of the wood is not considered. For further details, see Appendix A.

4.2. Lateral stiffness

According to EN 1995-1-1 [31], the stiffness under service load of laterally-loaded bolts is given per shear plane and fastener by Eq. (45) (units: $K_{ser,v}$ in N/mm, d in mm, ρ_m in kg/m^3):

$$K_{ser,v} = \frac{{\rho_m}^{1.5} \cdot d}{23} \tag{45}$$

Laterally-loaded bolts typically show an initial soft behaviour because they are inserted in oversized holes and EN 1995-1-1 [31] requires that the clearance should be added to the deformation calculated by the stiffness value given by Eq. (45). For laterally loaded threaded rods, the initial soft behaviour will presumably not be as severe as in bolts, due to continuous interlocking between the thread and the surrounding wood. Eq. (45) provides the combined lateral stiffness of two connected timber members in a timber-to-timber connection. Assuming symmetry (i.e. that the stiffness values the two connected members are equal), the stiffness per connected member is twice the value obtained by Eq. (45). EN 1995-1-1 [31] does not specify which value of the diameter should be used in Eq. (45). By use of the effective diameter d_{ef}, the lateral stiffness **per connected member** becomes:

$$K_{ser,v} = 2 \cdot \frac{{\rho_m}^{1.5} \cdot d_{ef}}{23} \tag{46}$$

Eq. (46) does not consider a series of parameters which presumably affect the stiffness, for example the angle β or the penetration length. Moreover, the loading configuration is not considered, e.g. whether the rotation of the rod is free or fixed or whether the lateral load is applied with eccentricity resulting in a moment. To study the influence of these parameters, the embedded part of a laterally loaded threaded rod may be represented as a beam on elastic foundation, as shown in Fig. 10c. It is assumed that the behaviour of the rod and the foundation is always linear-elastic. Any initial soft behaviour is neglected in this analysis. A more detailed analysis is given in Appendix A.

The analytical results in Appendix A suggest that the moment M_0 has a significant influence on the lateral stiffness. On the other hand, the analysis in Appendix A shows that the lateral stiffness $K_{ser,v,0}$ converges to its upper value for penetration lengths $l \geq 4 - 5 \cdot d$. Setting $n_{M0} = M_0 / F_v \cdot l_c$, the convergent stiffness of a semi-infinite rod ($l \to \infty$) is given by Eq. (47). Therefore, for the minimum penetration length of $6 \cdot d$ according to EN 1995-1-1 [31], the convergent stiffness for semi-infinite rods given by Eq. (47) can be used without significant loss in accuracy.

$$K_{ser,v,0}\,|_{l \to \infty} = \frac{k_v \cdot l_c}{2 + 2 \cdot n_{M0}} \tag{47}$$

The deflection at the loading point A depends on whether the rotation at the loading point is allowed or fixed, see Fig. 10d. Depending on this boundary condition, the total vertical stiffness of a laterally-loaded threaded rod with respect to the deflection at point A is given as follows:

- Free rotation at point A (re-formulating expression found in [55]):

$$K_{ser,v,tot} = \frac{3 \cdot k_v \cdot l_c}{4 \cdot {\lambda_0}^3 + 12 \cdot {\lambda_0}^2 + 12 \cdot \lambda_0 + 6} \tag{48}$$

- Fixed rotation at point A:

$$K_{ser,v,tot} = \frac{3 \cdot k_v \cdot l_c}{{\lambda_0}^3 + 3 \cdot {\lambda_0}^2 + 3 \cdot \lambda_0 + 3} \tag{49}$$

The term λ_0 is the length of the non-embedded part $l_0$of the rod normalized by l_c:

$$\lambda_0 = l_0 / l_c \tag{50}$$

The foundation modulus of laterally-loaded threaded rods remains unknown and experimental results are required. However, some conclusions may be drawn by experimental results from embedment tests of dowels with diameters comparable to the core diameters of threaded rods. Table 3 provides experimental results for the foundation modulus of dowels with diameters 12–16 mm at reference moisture content ($MC \approx 10-12\%$). The results in Table 3 come from different test set-ups, diameters and wood species and should only be treated as indicative.

The experimental values in Table 3 are much higher than the values estimated by Eq. (30). The foundation modulus of large-diameter dowels seems to depend on the diameter to a much greater degree than Eq. (30) suggests, especially for loading parallel to grain ($\beta = 0^\circ$). This is evident in the results by Karagiannis et al. 2016 [56] for dowels tested with the same set-up. Compared to 12 mm-dowels, the foundation modulus of 16 mm-dowels was 2.75 and 1.76 times higher for loading parallel and perpendicular to grain, respectively. Moreover, the experimental results in Table 3

Table 3
Embedment test results for dowels embedded in softwoods ($MC \approx 10-12\%$).

Source	β = 0° $k_{v,0}$(N/mm^2)	β = 90° $k_{v,90}$(N/mm^2)
Gattesco 1998 [57][a] East. alps spruce, $\rho_m \approx 470$ kg/m^3, d =16 mm, l = 30 mm	1209 (CoV =12.3%)	763 (CoV = 22.2%)
Santos et al. 2010 [58] Pine (*Pinus pinaster*), $\rho_m \approx 550 - 570$kg/m^3 d = 14 mm, l = 30 mm	1586 (CoV = 20.7%)	521 (CoV =23.7%)
Karagiannis et al. 2016 [56] Norway Spruce (*Picea abies*), $\rho_m \approx 430$ kg/m^3 d =12/16 mm, l = 40 mm	d =12: 376 (CoV = 15.4%) d =16: 1034 (CoV =17.3%)	d =12: 137 (CoV =30.7%) d =16: 241 (CoV =7.1%)
Application of Eq. (30) for threaded rods ρ = 430 kg/m^3, d =20 mm	215	184

[a] Mean result from configurations with and without lateral confinement.

show that the foundation modulus is dependent on the angle β, as higher values are obtained for parallel to grain loading ($\beta = 0^{\circ}$) compared to the corresponding values for perpendicular to grain loading ($\beta = 90^{\circ}$). This difference is greater than the one suggested by factor 1.17 in Eq. (30).

5. Combined axial and lateral loading

Fig. 11 shows a threaded rod subjected to axial and lateral loading. According to EN 1995-1-1 [31], a quadratic failure criterion applies for screws subjected to combined axial and lateral loading:

$$\left(\frac{F_{ax,Ed}}{F_{ax,Rd}}\right)^2 + \left(\frac{F_{v,Ed}}{F_{v,Rd}}\right)^2 \leq 1 \tag{51}$$

As an alternative to Eq. (51), the following expression may be used [55]:

$$F_{Ed} \leq F_{ax,Rd} \cdot \sin\alpha + F_{v,Rd} \cdot \cos\alpha \tag{52}$$

For inclined fasteners subjected to combined loading, stresses cannot fully develop near the edge (due to very small edge distance) and therefore they may be neglected for a certain length of the fastener, see in detail [59]. Based on mean values, both Eqs. (51) and (52) have shown good agreement with experimental results [55] for threaded rods ($d = 20$ mm) inserted in glulam at an angle 45–90°. On the contrary, Eq. (51) provided conservative predictions for self-tapping screws inserted perpendicular to grain in spruce, as shown in the experimental study by Laggner et al. [60], where the exponent was found equal to 2.4 for mean values and 3.1 for 5%-fractile values. In connections with fasteners subjected to combined axial and lateral loading, the direction of the displacement vector does not coincide with the direction of the applied force, as shown in Fig. 11. Therefore, it is not possible to fully model a threaded rod solely by use of a single spring element in the force direction (as also stated in [60]). Instead, assigning a spring element to each degree of freedom as shown in Fig. 11 is a more accurate description of the fastener.

6. Concluding remarks

This paper investigates the strength and stiffness properties for threaded rods with wood screw threads. Design guilelines by Eurocode 5 (EN 1995-1-1[31]) and European Technical Assessments and existing literature were reviewed to identify knowledge gaps and provide some proposals for improvement. The following main conclusions are drawn:

- A collection of experimental results was used to evaluate the existing rules in EN 1995-1-1 [31] and ETAs and derive simple expressions for the withdrawal capacity and stiffness.
- To the knowledge of the authors, the existing design rules with respect to buckling of self-tapping screws have not been experimentally verified for threaded rods.
- Test results for self-tapping screws indicate that the effective number of fasteners given by EN 1995-1-1 [31] ($n_{ef} = n^{0.9}$) is on the safe-side. This is yet to be fully verified for threaded rods. To the knowledge of the authors, there is no systematic experimental study of the block/plug shear capacity in configurations with multiple axially-loaded threaded rods.
- Theoretical expressions for laterally loaded threaded rods were provided. The lack of experimental results for laterally-loaded threaded rods was highlighted. Testing is required to obtain the embedment properties of laterally-loaded threaded rods (e.g. foundation modulus, embedment strength, effective diameter) and also to verify the derived theoretical expressions.
- The effects of moisture and load duration on the properties of screwed-in threaded rods remains largely unknown.
- The existing expressions for the design steel tensile capacity of threaded rods are probably very conservative.

Declaration of Competing Interest

The authors declare that they have no known competing financial interests or personal relationships that could have appeared to influence the work reported in this paper.

Acknowledgements

The financial support by the Research Council of Norway, Norway through WoodSol project (NFR grant no. 254699/E50) is gratefully acknowledged. The authors would like to thank H.J. Blaß, and O. Krüger for sharing details from their experimental campaign.

Credit author statement

Both authors have seen and approved the manuscript and have contributed significantly to its preparation. The 1st author has taken the initiative for the paper, written the paper (including figure preparation), developed the concepts/content and performed all calculations. The 2nd author has contributed to the concept/content development and has critically reviewed the manuscript.

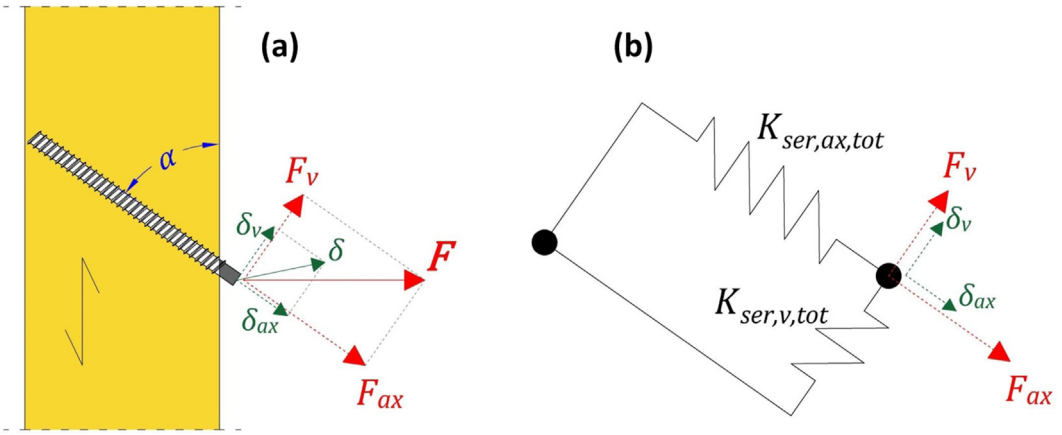

Fig. 11. Threaded rod subjected to combined axial and lateral loading: (a) forces and displacements, (b) modelling principle.

Appendix A. Modelling of a laterally-loaded threaded rod as a beam on elastic foundation

Fig. 10c shows the representative model of the embedded part of a laterally-loaded threaded rod as a beam on elastic foundation. It is assumed that the behaviour of the rod and the foundation is linear-elastic. The governing differential equation for the transverse displacement v is:

$$\frac{d^4 v}{dx^4} + \frac{4}{l_c^4} \cdot v = 0 \tag{A.1}$$

The term l_c is a characteristic length:

$$l_c = \sqrt[4]{4 \cdot E_s \cdot I_s / k_v} \tag{A.2}$$

The following definition is made:

$$\lambda = 2 \cdot l / l_c \tag{A.3}$$

The solution of Eq.(A.1) depends on the loading configuration and the boundary conditions (e.g. on the applied moment at the entrance point or whether rotation of the rod is allowed or not in these points). The full derivation of the expressions is cumbersome and is omitted herein. By setting $n_{M0} = M_0 / F_v \cdot l_c$, the vertical stiffness $K_{ser,v,0}$ at $x = 0$ is given by:

$$K_{ser,v,0} = \frac{k_v \cdot l_c}{2} \cdot \frac{\cosh\lambda - 2 + \cos\lambda}{(\sinh\lambda - \sin\lambda) + n_{M0} \cdot (\cosh\lambda - \cos\lambda)} \tag{A.4}$$

The term $n_{M0} = M_0 / F_v \cdot l_c$takes into account the effect of the moment M_0.

In the special case where rotation is restrained at $x = 0$, i.e. for $v'(0) = 0$, the moment reaction is given by Eq. (A.5) and the vertical stiffness by Eq. (A.6).

$$v'(0) = 0 \rightarrow M_{0,fixed} = -\frac{F_v \cdot l_c}{2} \cdot \frac{\cosh\lambda - \cos\lambda}{\sinh\lambda + \sin\lambda} \tag{A.5}$$

$$v'(0) = 0 \rightarrow K_{ser,v,0,fixed} = k_v \cdot l_c \cdot \frac{\sinh\lambda + \sin\lambda}{\cosh\lambda + 2 + \cos\lambda} \tag{A.6}$$

For a semi-infinite threaded rod ($l \rightarrow \infty$), the stiffness converges to:

$$K_{ser,v,0}\,|_{\lambda\rightarrow\infty} = \frac{k_v \cdot l_c}{2 + 2 \cdot n_{M0}} \tag{A.7}$$

In the special case of fixed end rotation at $x = 0$ for a semi-infinite rod, the moment reaction is equal to $M_{0,fixed} = -F_v \cdot l_c/2$, i.e. $n_{M0} = -1/2$.

Fig. A1 shows the predictions of Eq. (A.4) for $K_{ser,v,0}$ as function of the penetration length for a threaded rod with $d = 20$ mm and $d_1 = 15$ mm. The predictions are given for fixed rotation at entrance point (Eq. (A.6)) and for 3 different values of moment M_0: forn_{M0} = 0 (zero moment), 0.5 and 1.0. Two values for the foundation modulus were used to simulate different angles to grain. For a lateral loading parallel to grain ($\beta = 0^\circ$), $k_v = 1200$ N/mm^2 is used, while for lateral loading perpendicular to grain ($\beta = 90^\circ$), $k_v = 500$ N/mm^2 is used. These are crude approximations based on the experimental results given in Table 3. Finally, the prediction by EN1995-1-1 [31], i.e. Eq. (46), is provided assuming $\rho_m = 430$ kg/m^3 and $d_{ef} = 1.1 \cdot d_1$. As shown in Fig. A1, both the values of k_v and M_0 have a significant influence on the vertical stiffness. For the same foundation modulus, the results differ by a factor up to approx. 4, depending on the loading conditions (which can be further increased if higher moment is applied, i.e.n_{M0} > 1). EN1995-1-1 [31] do not account for these parameters and provides a single value. Finally, Fig. A1 shows that stiffness converges to the value given by Eq. (A.7) for penetration lengths $l \geq 4 - 5 \cdot d$.

For a laterally-loaded threaded rod subjected to eccentric loading ($l_0 > 0$) the moment distribution depends on whether rotation is restrained at the loading point A. Assuming for simplicity a semi-infinite rod, the following equations are obtained for the deflections and moments at point O and A for the corresponding boundary conditions (positive signs according to Fig. 10c and d):

- Free rotation at point A ($M_0 = F_v \cdot l_0$, $M_A = 0$, $V_0 = F_v$, $v'_{0,\text{freelength}} = v'_{0,\text{embeddedpart}}$)

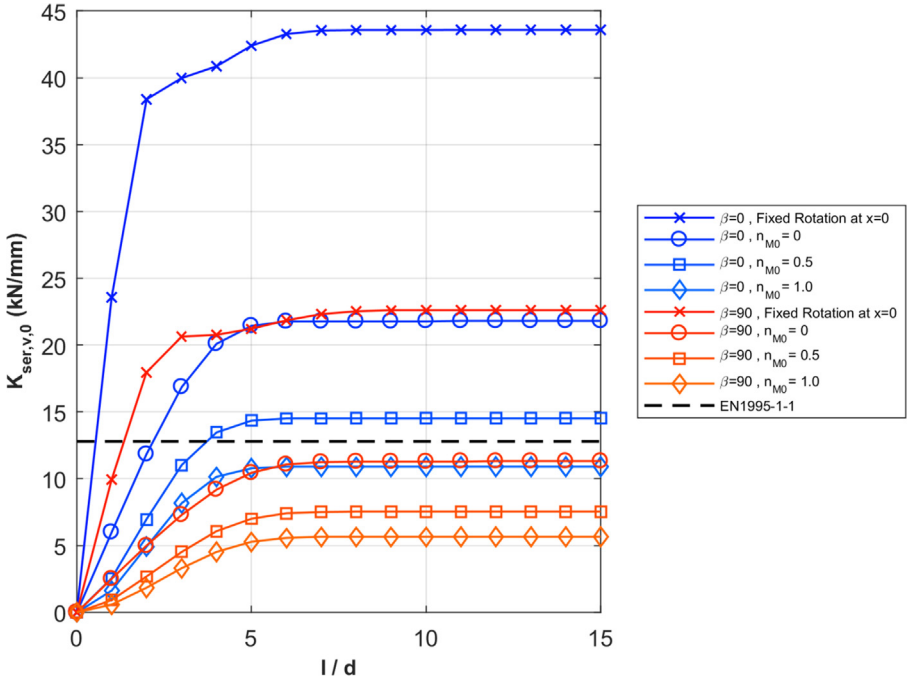

Fig. A1. Analytical prediction of Eq. (A.4) for vertical stiffness of a laterally loaded threaded rod in for varying k_v ($k_v = 1200$ N/mm^2 for $\beta = 0^\circ$ and $k_v = 500$ N/mm^2 for $\beta = 90^\circ$) and varying loading conditions. Rod with $d = 20$ mm and $d_1 = 15$ mm and$\rho_m = 430$ kg/m^3.

$$v_0 = \frac{2 \cdot (\lambda_0 + 1)}{k_v \cdot l_c} \cdot F_v \tag{A.8}$$

$$v_A = \frac{(4 \cdot {\lambda_0}^3 + 12 \cdot {\lambda_0}^2 + 12 \cdot \lambda_0 + 6)}{3 \cdot k_v \cdot l_c} \cdot F_v \tag{A.9}$$

- Fixed rotation at point A: $(V_0 = F_v, v'_A = 0, v'_{0,\text{freelength}} = v'_{0,\text{embeddedpart}})$

$$M_0 = \frac{F_v \cdot l_c}{2} \cdot (\lambda_0 - 1) = \frac{F_v}{2} \cdot (l_0 - l_c) \tag{A.10}$$

$$M_A = -\frac{F_v \cdot l_c}{2} \cdot (\lambda_0 + 1) = -\frac{F_v}{2} \cdot (l_0 + l_c) \tag{A.11}$$

$$v_0 = \frac{(\lambda_0 + 1)}{k_v \cdot l_c} \cdot F_v \tag{A.12}$$

$$v_A = \frac{({\lambda_0}^3 + 3 \cdot {\lambda_0}^2 + 3 \cdot \lambda_0 + 3)}{3 \cdot k_v \cdot l_c} \cdot F_v \tag{A.13}$$

Note that the deflections given by Eqs. (A.8) and (A.12) can be obtained by use of Eq. (A.7) by use of $n_{M0} = \lambda_0$ and $n_{M0} = (\lambda_0 - 1)/2$, respectively.

References

[1] K.A. Malo, H. Stamatopoulos, Connections with threaded rods in moment resisting frames, Proceedings of WCTE 2016 - World Conference on Timber Engineering, Vienna, Austria, 2016.

[2] K. Lied, K. Nordal, A conceptual study of glulam connections using threaded rods and connecting circular steel profiles, M.Sc. Thesis, NTNU Norwegian University of Science and Technology, Trondheim, Norway, 2016.

[3] M. Cepelka, K.A. Malo, Moment resisting on-site splice of large glulam elements by use of mechanically coupled long threaded rods, Eng. Struct. 163 (2018) 347–357.

[4] A. Vilguts, K.A. Malo, H. Stamatopoulos, Moment resisting frames and connections using threaded rods in beam-to column timber joints Proceedings of WCTE 2018 - World Conference on Timber Engineering, Seoul, Republic of Korea, 2018.

[5] K. Komatsu, T. Morimoto, S. Kurumada, H. Tanaka, T. Shimizu, S. Kawahara, N. Akiyama, M. Nakatani, Development of glulam moment-resisting joint having high initial stiffness, clear yielding moment and rich ductility Proceedings of WCTE 2018 - World Conference on Timber Engineering, Seoul, Republic of Korea, 2018.

[6] G. Pirnbacher, R. Brandner, G. Schickhofer, Base parameters of self-tapping screws, Proceedings of the 42nd CIB-W18 meeting Dübendorf, Switzerland, 2009.

[7] M. Frese, H.J. Blaß, Models for the calculation of the withdrawal capacity of self-tapping screws, Proceedings of the 42nd CIB-W18 meeting Dübendorf, Switzerland, 2009.

[8] A. Ringhofer, R. Brandner, G. Schickhofer, A universal approach for withdrawal properties of self-tapping-screws in solid timber and laminated timber products, Proceedings of the 2nd INTER meeting Šibenik, Croatia, 2015.

[9] S. Kennedy, A. Salenikovich, W. Munoz, M. Mohammad, Design equation for withdrawal resistance of threaded fasteners in the Canadian timber design code, Proceedings of WCTE 2014 - World Conference on Timber Engineering, Quebec City, Canada, 2014.

[10] U. Hübner, Withdrawal strength of self-tapping screws in hardwoods, Proceedings of the 46th CIB-W18 meeting Vancouver, Canada, 2013.

[11] H.J. Blaß, I. Bejtka, T. Uibel, Tragfähigkeit von verbindungen mit selbstbohrenden holzschrauben mit vollgewinde, Universitätsverlag Karlsruhe Karlsruhe, 2006.

[12] A. Ringhofer, R. Brandner, G. Schickhofer, Withdrawal resistance of self-tapping screws in unidirectional and orthogonal layered timber products, Mater. Struct./Mater. Constr. (2013) 1–13.

[13] R. Brandner, Properties of axially loaded self-tapping screws with focus on application in hardwood, Wood Mat. Sci. Eng. 14 (5) (2019) 254–268.

[14] E. Gehri, Influence of fasteners spacings on joint performance – Experimental results and codification, Proceedings of the 42nd CIB-W18 meeting Dübendorf, Switzerland, 2009.

[15] T. Uibel, H.J. Blaß, Determining suitable spacings and distances for self-tapping screws by experimental and numerical studies, Proceedings of WCTE 2010 – World Conference on Timber Engineering, Riva del Garda, Trentino, Italy, 2010, pp. 3204-3212.

[16] D. Carradine, P. Newcombe, A. Buchanan, Using screws for structural applications in laminated veneer lumber, Proceedings of the 42nd CIB-W18 meeting Dübendorf, Switzerland, 2009.

[17] U. Mahlknecht, R. Brandner, Block shear failure mechanism of axially-loaded groups of screws, Eng. Struct. 183 (2019) 220–242.

[18] U. Mahlknecht, R. Brandner, A. Ringhofer, G. Schickhofer, Resistance and Failure Modes of Axially Loaded Groups of Screws, in: S. Aicher, H.W. Reinhardt, H. Garrecht (Eds.), Materials and Joints in Timber Structures-Recent Developments of Technology, Springer: RILEM Bookseries 2014, pp. 289–300.

[19] ETA Danmark A/S, European Technical Approval ETA-12/0114, SPAX self-tapping screws, 2013.

[20] ETA Danmark A/S, European Technical Assessment ETA-11/0030 of 2019/10/08, Rotho Blaas s.r.l, 2019.

[21] ETA Danmark A/S, European Technical Assessment ETA-11/0024 of 02/03/2017, E.u.r.o. Tec GmbH, 2017.

[22] ETA Danmark A/S, European Technical Approval ETA-13/0090, NOVA self-tapping screws, 2013.

[23] H.J. Blaß, O. Krüger, Schubverstärkung von Holz mit Holzschrauben und Gewindestangen, KIT Scientific Publishing, Karlsruhe, 2010.

[24] H. Stamatopoulos, K.A. Malo, Withdrawal stiffness of threaded rods embedded in timber elements, Constr. Build. Mater. 116 (2016) 263–272.

[25] H. Stamatopoulos, K.A. Malo, Withdrawal capacity of threaded rods embedded in timber elements, Constr. Build. Mater. 94 (2015) 387–397.

[26] H. Stamatopoulos, K.A. Malo, Characteristic withdrawal capacity and stiffness of threaded rods, Proceedings of the 2nd INTER meeting Šibenik, Croatia, 2015.

[27] M. Nakatani, K. Komatsu, Development and verification of theory on pull-out properties of Lagscrewbolted timber joints, Proceedings of the 8th World Conference on Timber Engineering, Lahti, Finland, 2004, pp. 95–99.

[28] J.L. Jensen, M. Nakatani, P. Quenneville, B. Walford, A simple unified model for withdrawal of lag screws and glued-in rods, Eur. J. Wood Wood Prod. 69 (2011) 537–544.

[29] T. Mori, M. Nakatani, S. Kawahara, T. Shimizu, K. Komatsu, Influence of the number of fastener on tensile strength of lagscrewbolted glulam joint, Proceedings of the 10th World Conference on Timber Engineering, Miyazaki, Japan, 2008, pp. 1100–1107.

[30] H. Stamatopoulos, K.A. Malo, Withdrawal of pairs of threaded rods with small edge distances and spacings, Eur. J. Wood Wood Prod. 76 (1) (2018) 31–42.

[31] CEN, NS-EN 1995-1-1:2004+A1:2008+A2:2014, Design of timber structures - Part 1-1: General - Common rules and rules for buildings, European committee for standarization, Brussels.

[32] CEN, EN 14592:2008+A1:2012: Timber structures- Dowel type fasteners-Requirements, European Committee for Standardization, Brussels, Belgium, 2012.

[33] H. Stamatopoulos, Withdrawal properties of threaded rods embedded in glued-laminated timber elements, Ph.D. Thesis, Department of Structural Engineering, Norwegian University of Science and Technology, Trondheim, Norway, 2016.

[34] M. Stepinac, F. Hunger, R. Tomasi, E. Serrano, V. Rajcic, J.W.G. Van De Kuilen, Comparison of design rules for glued-in-rods and design rule proposal for implementation in European standards, Proceedings of the 46th CIB-W18 meeting Vancouver, Canada, 2013.

[35] R. Steiger, E. Serrano, M. Stepinac, V. Rajčić, C. O'Neill, D. McPolin, R. Widmann, Strengthening of timber structures with glued-in rods, Constr. Build. Mater. 97 (2015) 90–105.

[36] P. Dietsch, Reinforcement of timber structures - Standardization towards a new section for EC5, in: J. Branco, E. Poletti, H. Sousa (Eds.) SHATIS19, 5th International Conference on Structural Health Assessment of Timber Structures, Universidade do Minho, Guimarães, Portugal, 2019.

[37] CEN, NS-EN 1993-1-1:2005+A1:2014+NA:2015. Eurocode 3, Design of steel structures - Part 1-1: General rules and rules for buildings, European Committee for Standardization, Brussels, Belgium, 2015.

[38] H.J. Blaß, I. Bejtka, Reinforcements perpendicular to grain using self-tapping screws, Proceedings of the 8th World Conference on Timber Engineering, Lahti, Finland, 2004, pp. 233–238.

[39] DIN, Deutsches Institut für Normung, DIN 7998:Gewinde und Schraubenenden für Holz-schrauben, Berlin, Germany, 1975.

[40] SFS intec, GmbH, Gewindestangen mit Holzgewinde als Holzverbindungsmittel, Allgemeine bauaufsichtliche Zulassung Z-9.1-777, Deutsches Institut für Bautechnik (DIBt), 2010.

[41] CEN, EN 384:2016+A1:2018 - Structural timber - Determination of characteristic values of mechanical properties and density, European Committee for Standardization, Brussels, Belgium, 2018.

[42] CEN, EN 14358:2016: Timber Structures: Calculation and verification of characteristic values, European Committee for Standardization, 2016.

[43] O. Volkersen, Die nietkraftverteilung in zugbeanspruchten nietverbindungen mit konstanten laschenquerschnitten, Luftfahrtforschung 15 (1938) 41–47.

[44] M. Cepelka, K.A. Malo, Moment resisting splice of timber beams using long threaded rods and grout-filled couplers – Experimental results and predictive models, Constr. Build. Mater. 155 (2017) 560–570.

[45] G. Pirnbacher, G. Schickhofer, Zeitabh¨angige Entwicklung der Traglast und Kriechver-halten von axial beanspruchten selbstbohrenden Holzschrauben, COMET Area-Meeting, Graz, Austria, 2012.

[46] A. Ringhofer, M. Grabner, C. Silva, M. Branco, G. Schickhofer, The influence of moisture content variation on the withdrawal capacity of self-tapping screws, Holztechnologie 55 (3) (2014) 33–40.

[47] J.L. Jensen, A. Koizumi, T. Sasaki, Y. Tamura, Y. Iijima, Axially loaded glued-in hardwood dowels, Wood Sci. Technol. 35 (2001) 73–83.
[48] H. Larsen, Rigid connections in glulam beams, M.Sc. Thesis, Norwegian University of Science and Technology, Trondheim, Norway, 2012.
[49] I. Bejtka, Verstärkung von Bauteilen aus Holz mit Vollgewindeschrauben, Universitätsverlag Karlsruhe Karlsruhe, 2005.
[50] H. Krenn, G. Schickhofer, Joints with inclined screws and steel plates as outer members, Proceedings of the 42nd CIB-W18 meeting Dübendorf, Switzerland, 2009.
[51] E. Gonzalez, C. Avez, T. Tannert, Timber joints with multiple glued-in steel rods, J. Adhesion 92 (7–9) (2016) 635–651.
[52] J.M. Cabrero, M. Yurrita, A review of the existing models for brittle failure in connections loaded parallel to the grain, in: C. Sandhaas, J. Munch-Andersen, P. Dietsch (Eds.), Design of Connections in Timber Structures: A state-of-the-art report by COST Action FP1402 / WG3 Shaker Verlag GmbH, Aachen, Germany, 2018, pp. 127–141.
[53] K.W. Johansen, Theory of timber connectors, International Association of Bridges and Structural Engineering, Bern, Switzerland 1949, pp. 249–262.
[54] H. Riberholt, Glued bolts in glulam – Proposals for CIB code, Proceedings of the 21st CIB-W18 meeting Parksville, Canada, 1988.
[55] M. Cepelka, K.A. Malo, H. Stamatopoulos, Effect of rod-to-grain angle on capacity and stiffness of axially and laterally loaded long threaded rods in timber joints, Eur. J. Wood Wood Prod. 76 (4) (2018) 1311–1322.
[56] V. Karagiannis, C. Málaga-Chuquitaype, A.Y. Elghazouli, Modified foundation modelling of dowel embedment in glulam connections, Constr. Build. Mater. 102 (2016) 1168–1179.
[57] N. Gattesco, Strength and local deformability of wood beneath bolted connectors, J. Struct. Eng. 124 (2) (1998) 195–202.
[58] C.L. Santos, A.M.P. De Jesus, J.J.L. Morais, J.L.P.C. Lousada, A comparison between the EN 383 and ASTM D5764 test methods for dowel-bearing strength assessment of wood: experimental and numerical investigations, Strain 46 (2) (2010) 159–174.
[59] R. Jockwer, R. Steiger, A. Frangi, Fully Threaded Self-tapping Screws Subjected to Combined Axial and Lateral Loading with Different Load to Grain Angles, in: S. Aicher, H.W. Reinhardt, H. Garrecht (Eds.), Materials and Joints in Timber Structures - Recent Developments of Technology, RILEM Bookseries, 2014, pp. 265–272.
[60] T. Laggner, G. Flatscher, G. Schickhofer, Combined loading of self-tapping screws, Proceedings of WCTE 2016 - World Conference on Timber Engineering, Vienna, Austria, 2016.